Estimation of Radiation Exposure of 128-Slice 4D-Perfusion CT for the Assessment of Tumor Vascularity

Dominik Ketelsen, MD[1]
Marius Horger, MD[1]
Markus Buchgeister, MD[2]
Michael Fenchel, MD[1]
Christoph Thomas, MD[1]
Nadine Boehringer, MS[1]
Maximilian Schulze, MD[1]
Ilias Tsiflikas, MD[1]
Claus D. Claussen, MD[1]
Martin Heuschmid, MD[1]

Index terms:
Perfusion CT
Tumor vascularity
Radiation exposure
Effective dose
128-slice CT
Alderson-Rando phantom

DOI:10.3348/kjr.2010.11.5.547

Korean J Radiol 2010;11:547-552
Received February 11, 2010; accepted after revision June 3, 2010.

[1]Department of Diagnostic and Interventional Radiology, University Hospital Tuebingen, Hoppe-Seyler-Strasse 3, 72076 Tuebingen, Germany; [2]Departments of Radiotherapy and Radiooncology, University Hospital Tuebingen, Hoppe-Seyler-Strasse 3, 72076 Tuebingen, Germany

Corresponding author:
Dominik Ketelsen, MD, Department of Diagnostic and Interventional Radiology, Eberhard-Karls-University Tuebingen, Hoppe-Seyler-Strasse 3, 72076 Tuebingen, Germany.
Tel. 49 7071 2986677
Fax. 49 7071 29 4478
e-mail: dominik.ketelsen@med.uni-tuebingen.de

Objective: We aimed to estimate the effective dose of 4D-Perfusion-CT protocols of the lung, liver, and pelvis for the assessment of tumor vascularity.

Materials and Methods: An Alderson-Rando phantom equipped with thermoluminescent dosimeters was used to determine the effective dose values of 4D-Perfusion-CT. Phantom measurements were performed on a 128-slice single-source scanner in adaptive 4D-spiral-mode with bidirectional table movement and a total scan range of 69 mm over a time period of nearly 120 seconds (26 scans). Perfusion measurements were simulated for the lung, liver, and pelvis under the following conditions: lung (80 kV, 60 mAs), liver (80 kV/80 mAs and 80 kV/120 mAs), pelvis (100 kV/80 mAs and 100 kV/120 mAs).

Results: Depending on gender, the evaluated body region and scan protocol, an effective whole-body dose between 2.9–12.2 mSv, was determined. The radiation exposure administered to gender-specific organs like the female breast tissue (lung perfusion) or to the ovaries (pelvic perfusion) led to an increase in the female specific dose by 86% and 100% in perfusion scans of the lung and the pelvis, respectively.

Conclusion: Due to a significant radiation dose of 4D-perfusion-CT protocols, the responsible use of this new promising technique is mandatory. Gender- and organ-specific differences should be considered for indication and planning of tumor perfusion scans.

Perfusion CT was introduced several years ago as an adjunct to morphological imaging in tumor patients. Considering tumor perfusion as an *in vivo* marker of angiogenesis, the first studies showed reliable results for diagnosis, risk-stratification, and therapy monitoring of several tumor entities (1). This functional imaging technique has emerged as a new tool in the evaluation of blood supply and perfusion characteristics in the oncological field. For example, in colorectal cancer, the second most common cancer in the western world, the main mechanism activating neovascularization is angiogenesis, which is the growth of new blood vessels. Neovascularization arises early via the upregulation of several angiogenetic factors. Thus, the assessment of the tumor microvascularity by perfusion CT could play an important role in the management of oncologic patients (2). The first clinical trials suggest that merely using tumor size is not sufficient for monitoring modern anti-angiogenesis drugs. In contrast, the functional information of perfusion CT could be used to monitor anti-angiogenesis therapy, which is increasingly used in oncologic therapy (1, 3).

The introduction of a new 128-slice single source scanner technique allows for oncologic perfusion imaging with its inherent possibility of 4D spiral scanning. This is

implemented by bidirectional table movements and broad detector range, resulting in coverage of organs and tumors up to a craniocaudal extent of 96 mm. On the other hand, modern tube techniques allow constant image quality over a time period of 120 seconds. However, in younger oncologic patients, the radiation exposure originating from additional spiral scans for tumor diagnosis or follow-up has to be considered. To the best of the authors' knowledge, no recent data is available, regarding the evaluation of effective whole-body and organ specific doses of 4D spiral scanning using a single source 128-slice scanner.

The aim of this study was to estimate gender specific effective whole-body and organ-specific doses when using 4D perfusion protocols for the lung, liver, and pelvis in normal-weighted and obese patients. The experimental dose measurements may lend support for consideration of new dose-balanced anatomo-functional CT imaging protocols that are dose neutral with existing oncologic CT investigational protocols.

MATERIALS AND METHODS

Dosimetry

Dose measurements were performed using an anthropomorphic phantom (Alderson-Rando-Phantom; Alderson Research Laboratories Inc., Stanford, CT) equipped with 117 thermoluminescent dosimeters (TLDs) measuring 1 × 1 × 6 mm (TLD-100H, Bicon-Harshow, Radiation Measurement Products, Cleveland, OH) (Fig. 1) (4–6).

Thirty-nine different positions in the Alderson-Rando-Phantom corresponding to the anatomical position of each individual organ were used for determining organ dose. Three TLDs were placed at each point of dose measurement to minimize bias due to measurement deviation. The number of TLDs allocated to different organ position were as follows: three at the brain, thyroid gland, esophagus, thymus, heart, breast, stomach, upper colon, spleen, kidneys, adrenal glands, pancreas, small intestine, lower colon, urinary bladder, muscle tissue, red bone marrow, skin, ovaries and testicles, 42 at the lung, and 15 at the liver. In organs which exist in pairs, the TLDs were positioned on the right side.

The evaluation of the irradiated TLDs (within 24 hour after exposure) was performed using a TLD reader (Model 5500 TLD Reader, Bicron Radiation Measurement Products, Solon, OH). The readout TLD values in nanocoulombs were multiplied by an individual calibration factor, which was defined by the means of parallel exposure in 33 TLDs, multiplied by a known radiation dose using 100 kV and 80 mA for 100 ms at an SSD of 100 cm (Elektra PreciseSim X-ray simulator, Stockholm, Sweden). To minimize the heel effect, wire markers in the field were avoided and all exposures were administered in the same position with respect to the orientation of the X-ray tube. The reference TLDs were exposed with a dose of 1.055 mGy and crosschecked by an ionization dosimeter positioned at the same phantom depths. No further correction factors were used since the calibration voltage was close to the CT's tube voltage (4).

The effective dose was calculated according to the guidelines of International Commission on Radiological Protection (ICRP) 103 by summarizing the weighted organ doses (7); the radiation dose of simulated small organs (i.e., thyroid gland) were directly rated into the calculation

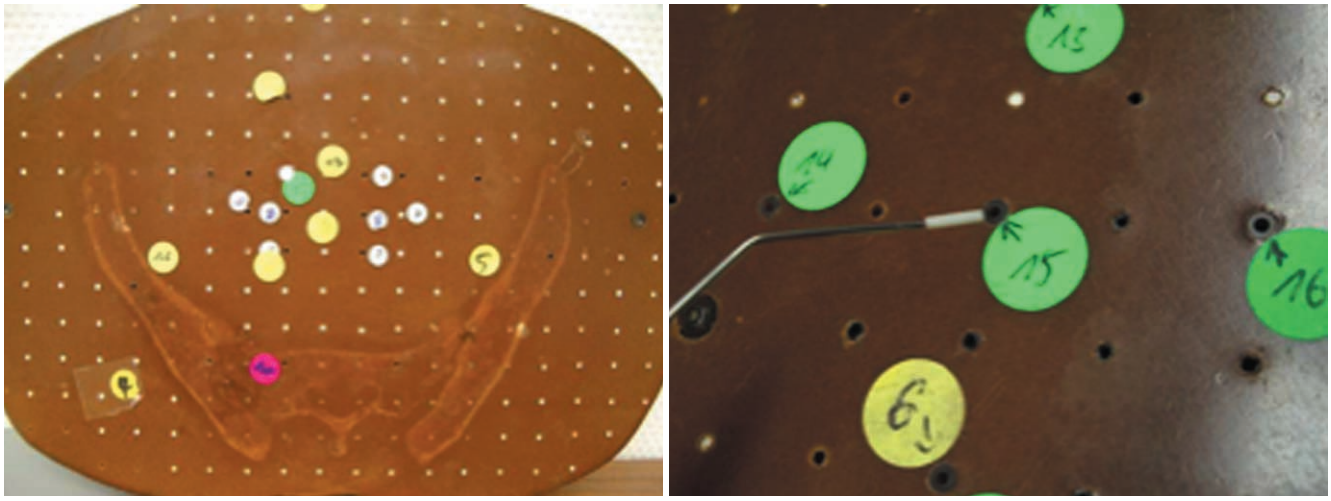

A **B**

Fig. 1. Dosimeters and dosimetry.
A, B. One 25 mm slice of 35 layers (**A**) of Alderson-Rando phantom at pelvis, with numbering of borehole positions representing pelvic organs. TLD is positioned to defined borehole with aid of vacuum forceps (**B**).

(mean of measured TLDs). Doses for larger organs (i.e., lung) were determined by determining the mean of measured TLDs from the entire organ.

To assess gender-specific differences, the testicles were used to measure the male-specific gonad dose while radiation dose of the breast and ovaries accounted for the female-specific radiation exposure.

Scan Protocols

For all CT examinations, a 128-slice single source scanner was used (SOMATOM Definition AS+, Siemens Medical Solutions, Forchheim, Germany). Data acquisition was performed in the supine position using a topogram to determine the examination scan range. Scans of three different organ regions were measured: one protocol was centered at the pulmonary hilum, one at the liver, and one at the pelvic inlet. To date, no consensus of the perfusion CT protocols has emerged (1). Therefore, the following protocols for normal weight (body mass index < 30 kg/m^2) and obese patients (body mass index > 30 kg/m^2) were chosen according to recent research guidelines of manufacturer and first clinical experiences in our institution (8–13): 128 × 0.6 mm collimation, rotation time 0.30 sec, scan range of 69 mm. The specific protocol parameters are listed in Table 1. For the 4D scanning mode, repeated 3D scans were used to monitor both the first pass and subsequent phases of tumor perfusion, which was determined by the contrast material in the intravascular and extravascular compartments (1, 2, 14): first phase, 10 scans every 2 seconds, second phase, 10 scans every 3 seconds and third phase, 6 scans every 10 seconds beginning after a start delay of 5, 7 and 9 seconds after contrast media application (50 ml) for the lung, liver, and pelvis perfusion, respectively.

For the first phase, body perfusion software (Siemens Medical Solutions, Forchheim, Germany) uses the one-compartment method to analyze the perfusion images during the first pass to calculate blood flow, expressed in a unit of ml/100 ml/min. In the interstitial phase, the blood volume (ml/100 ml) is calculated by the two-compartment or Patlak's method to measure the blood flowing in the tissue. Permeability (ml/100 ml/min) is analyzed by the transit constant (K^{trans}) using Patlak's method and measured the fraction of contrast media at the end of the arterial capillaries in relation to the potential to diffuse into the extravascular and extracellular space respectively (11).

To avoid unnecessary X-ray radiation remote of the clinically relevant area being scanned, the so called z-overscanning, a new adaptive dose shield technique was performed in this 128-slice scanner for all scan protocols.

RESULTS

Effective gender-specific dose perfusion protocols of the pulmonary hilum, liver, and the pelvic inlet are displayed in Table 2.

Using the lung perfusion protocol, organs within the range of the primary beam received effective organ doses of up to 3.0 mSv (breast tissue) or 2.9 mSv (lung tissue), respectively. In the liver perfusion protocol, significant doses were evident in liver tissue (1.1 mSv/1.5 mSv) and stomach (3.1 mSv/6.4 mSv) for normal weighted and obese patients. For the pelvic perfusion, significant organ doses were observed, especially in the region of the ovaries (3.0 mSv/6.1 mSv) and the urinary bladder (1.5 mSv/3.1 mSv) for the 80 and 120 mAs protocols.

The radiation dose applied to gender-specific organs such as the breast using the lung perfusion protocol or the ovaries in the pelvic perfusion protocol are responsible for

Table 2. Estimated Effective Dose of 4D Perfusion Protocols for Normal Weighted[1] and Obese[2] Males and Females

Protocol	Effective Dose Male (mSv)	Effective Dose Female (mSv)
1: Lung perfusion[1, 2]	3.5	6.5
2: Liver perfusion[1]	7.0	7.1
3: Liver perfusion[2]	11.9	12.2
4: Pelvic perfusion[1]	2.9	5.8
5: Pelvic perfusion[2]	5.5	11.5

Table 1. Specific Scan Parameters of 4D Perfusion Protocols of Lung (1), Liver (2, 3) and Pelvic Inlet (4, 5) for Normal Weighted[1] and Obese[2] Patients

Protocol	Tube Current	Tube Voltage	Total mAs	$CTDI_{Vol}$ (mGy)	DLP (mGy cm)
1[1, 2]	60 mAs	80 kV	2,336	21.62	186
2[1]	80 mAs	80 kV	1,914	16.71	144
3[2]	120 mAs	80 kV	4,768	44.90	386
4[1]	80 mAs	100 kV	2,222	40.12	345
5[2]	120 mAs	100 kV	4,802	95.11	817

Note.— CTDI = CT dose index, DLP = dose length product

the increase of the radiation dose in females (up to 86% or 100%) in both protocols (normal weight patients), respectively. Due to the lack of gender-specific organs in the scan range of the liver perfusion, the effective doses of males and females are comparable (Fig. 2) for normal weighted and obese patients (Table 3).

An increase in the tube current from 80 to 120 mAs was noted in protocols for obese patients led to a higher radiation dose (up to 109%) in females for the pelvic perfusion protocol.

DISCUSSION

Since it was demonstrated for several tumor entities that high values of tumor microvessel density and high vascular endothelial growth factor expression are associated with poor outcomes, the use of perfusion CT as an *in vivo* marker for angiogenesis has emerged as a promising tool for tumor diagnosis and therapy monitoring, especially due to the high reproducibility of quantitative perfusion imaging (15–20).

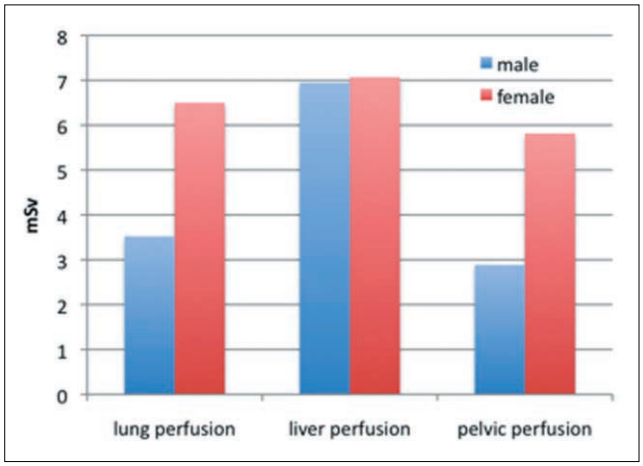

Fig. 2. Gender-specific estimated effective whole-body dose of different 4D perfusion protocols with scan range of 69 mm for normal weighted patients.

As no larger clinical trials evaluated the value of perfusion CT up to today, no standard protocols are available. Therefore, perfusion CT is usually performed as an add-on to the standard oncological whole-body scans for diagnosis, risk stratification, and therapy monitoring (2, 14, 15).

The radiation dose of additional CT scans is a cause of concern, especially in younger oncologic patients, due to the associated risk of developing secondary malignancies (21).

Due to the updated ICRP 103 tissue weighting factors, recent conversion coefficients based on ICRP 60, underestimate the effective dose compared to organ-dose-based calculations. Christner et al. (22) reported a 7% decrease in effective dose for CT examinations of the abdomen and pelvis, but did note an increased estimated effective dose of 4% and 14% for scans of the liver and chest, respectively, compared to the ICRP 60 based conversion coefficients. Furthermore, the updated weighting factor for the female breast (0.05 to 0.12) leads to an increased female-specific effective dose for thoracic examinations up to 31%, compared to ICRP 60 (23).

Depending on gender and the evaluated body region and protocols for normal weight or obese patients, an effective whole-body dose between 2.9 and 12.2 mSv was measured. Our data show an increase in effective radiation exposure in the area of respective scan range, whereas the additional radiation dose is relatively low outside of the

Table 3. Measured Organ Equivalent Doses of Different 4D Perfusion Protocols (mSv) for Normal Weighted[1] and Obese[2] Patients

Organ / Tissue	Lung[1, 2]	Liver[1]	Liver[2]	Pelvic[1]	Pelvic[2]
Thyroid gland	0.05	0.03	0.03	0.03	0.02
Esophagus	0.01	0.95	0.49	0.05	0.10
Lung	2.90	0.07	0.29	0.06	0.06
Breast	2.98	0.07	0.28	0.11	0.09
Stomach	0.21	3.12	6.41	0.12	0.21
Liver	0.12	1.11	1.51	0.04	0.06
Colon	0.01	0.15	0.23	0.70	1.45
Urinary bladder	0.00	0.03	0.02	1.52	3.07
Red bone marrow	0.04	0.01	0.06	0.00	0.01
Skeleton	0.00	0.00	0.01	0.00	0.00
Skin	0.01	0.00	0.00	0.00	0.00
Male gonads	0.00	0.00	0.01	0.21	0.19
Female gonads	0.00	0.05	0.04	3.03	6.13
Remaining organs	0.16	1.47	2.86	0.15	0.35

scan range. In perfusion protocols of the lung, the female effective dose increases by 86% (normal weighted patients) due to the radiation sensitive breast tissue located in the range of primary beam. Therefore, for younger women especially, the potential adverse effects regarding the life-time risk for breast cancer have to be considered. The measured perfusion of the pelvic inlet also showed an increase in female specific radiation dose by 100% (normal weighted patients) due to the ovarian tissue in the scan range. The highest measured effective whole body dose was observed performing a liver perfusion scan because of the stomach mucosa situated in the scan range. However, no gender-specific differences were evident in these cases.

The above mentioned gender- and organ-specific differences have to be considered in indicating and planning perfusion CT imaging.

Another aspect that has to be further evaluated in upcoming larger clinical trials are the specific optimization of scan parameters (i.e., tube current and tube potential for normal weighted and obese patients) in order to keep the radiation exposure as low as reasonably achievable, while providing reliable information about perfusion parameters such as organ or tumor blood flow, blood volume, mean transit time, and vascular permeability (24, 25). In this trial, the effective whole-body dose increases in the pelvic perfusion protocol for obese females by up to 109% in the 120 mAs protocol compared to the 80 mAs perfusion scan.

In the present study, tube current and tube potential was chosen according to the first clinical experiences in our institution. It has to be considered that radiation dose increases linearly with tube current. In contrast, tube potential changes cause a substantial change in radiation dose, which is proportional to the square root of the tube voltage (26).

Since radiation exposure also shows a linear dependence on the scan range, the possible scan range of 69 to 96 mm for 4D perfusion scanning has to be chosen responsibly and based on clinical relevance by an experienced radiologist (27). Other possibilities to control radiation exposure are to reduce the number of perfusion scans in order to reliably characterize the tissue response curve, which also has to be evaluated in further clinical trials.

In conclusion, the significant additional radiation exposure inherent with 4D perfusion scanning must be carefully weighed against the benefit of additional functional information, and demands a responsible use of this promising new technique. In particular, the development of combined dose-balanced anatomo-functional CT investigational protocols should gain priority, as the evaluation of response to treatment using perfusion measurements makes additional helicals (e.g., portal-venous, equilibrium phase) obsolete. Furthermore, the general clinical context (e.g., curative vs. palliative chemotherapy) is decisive for the appreciation of long term cancerous complications of increased CT-radiation exposure. Moreover, the evaluation of novel emerging antiangiogenic therapies makes perfusion measurements mandatory and one should keep in mind that CT is and will still remain the mainstay in the imaging diagnosis of oncologic patients and that adapted one-stop shop protocols combining whole-body screening in Care-dose technique and tumor focused perfusion data acquisition could represent a future solution for a more accurate evaluation of cancer patients.

References

1. Miles KA. Perfusion CT for the assessment of tumour vascularity: which protocol? *Br J Radiol* 2003;76:S36-S42
2. Wu GY, Ghimire P. Perfusion computed tomography in colorectal cancer: protocols, clinical applications and emerging trends. *World J Gastroenterol* 2009;15:3228-3231
3. Li WW. Tumor angiogenesis: molecular pathology, therapeutic targeting, and imaging. *Acad Radiol* 2000;7:800-811
4. Ketelsen D, Thomas C, Werner M, Luetkhoff MH, Buchgeister M, Tsiflikas I, et al. Dual-source computed tomography: estimation of radiation exposure of ECG-gated and ECG-triggered coronary angiography. *Eur J Radiol* 2010;73:274-279
5. Hunold P, Vogt FM, Schmermund A, Debatin JF, Kerkhoff G, Budde T, et al. Radiation exposure during cardiac CT: effective doses at multi-detector row CT and electron-beam CT. *Radiology* 2003;226:145-152
6. Ketelsen D, Luetkhoff MH, Thomas C, Werner M, Buchgeister M, Tsiflikas I, et al. Estimation of the radiation exposure of a chest pain protocol with ECG-gating in dual-source computed tomography. *Eur Radiol* 2009;19:37-41
7. The 2007 Recommendations of the International Commission on Radiological Protection. ICRP publication 103. *Ann ICRP* 2007;37:1-332
8. Ng QS, Goh V, Klotz E, Fichte H, Saunders MI, Hoskin PJ, et al. Quantitative assessment of lung cancer perfusion using MDCT: does measurement reproducibility improve with greater tumor volume coverage? *AJR Am J Roentgenol* 2006;187:1079-1084
9. Park MS, Klotz E, Kim MJ, Song SY, Park SW, Cha SW, et al. Perfusion CT: noninvasive surrogate marker for stratification of pancreatic cancer response to concurrent chemo- and radiation therapy. *Radiology* 2009;250:110-117
10. Ng CS, Wang X, Faria SC, Lin E, Charnsangavej C, Tannir NM. Perfusion CT in patients with metastatic renal cell carcinoma treated with interferon. *AJR Am J Roentgenol* 2010;194:166-171
11. Petralia G, Preda L, D'Andrea G, Viotti S, Bonello L, De Filippi R, et al. CT perfusion in solid-body tumours. Part I: technical issues. *Radiol Med* 2010 [Epub ahead of print]
12. Yang HF, Du Y, Ni JX, Zhou XP, Li JD, Zhang Q, et al. Perfusion computed tomography evaluation of angiogenesis in liver cancer. *Eur Radiol* 2010;20:1424-1430
13. Bellomi M, Viotti S, Preda L, D'Andrea G, Bonello L, Petralia G. Perfusion CT in solid body-tumours part II. Clinical applications and future development. *Radiol Med* 2010 [Epub ahead of

print]
14. Zhong L, Wang WJ, Xu JR. Clinical application of hepatic CT perfusion. *World J Gastroenterol* 2009;15:907-911
15. Bellomi M, Petralia G, Sonzogni A, Zampino MG, Rocca A. CT perfusion for the monitoring of neoadjuvant chemotherapy and radiation therapy in rectal carcinoma: initial experience. *Radiology* 2007;244:486-493
16. Cuenod CA, Fournier L, Balvay D, Guinebretière JM. Tumor angiogenesis: pathophysiology and implications for contrast-enhanced MRI and CT assessment. *Abdom Imaging* 2006;31:188-193
17. Kapanen M, Halavaara J, Hä kkinen AM. Comparison of liver perfusion parameters studied with conventional extravascular and experimental intravascular CT contrast agents. *Acad Radiol* 2007;14:951-958
18. Kudo M. Imaging blood flow characteristics of hepatocellular carcinoma. *Oncology* 2002;62:48-56
19. Petralia G, Preda L, Giugliano G, Jereczek-Fossa BA, Rocca A, D'Andrea G, et al. Perfusion computed tomography for monitoring induction chemotherapy in patients with squamous cell carcinoma of the upper aerodigestive tract: correlation between changes in tumor perfusion and tumor volume. *J Comput Assist Tomogr* 2009;33:552-559
20. Gillard JH, Antoun NM, Burnet NG, Pickard JD. Reproducibility of quantitative CT perfusion imaging. *Br J Radiol* 2001;74:552-555
21. Brenner DJ, Hall EJ. Computed tomography--an increasing source of radiation exposure. *N Engl J Med* 2007;357:2277-2284
22. Christner JA, Kofler JM, McCollough CH. Estimating effective dose for CT using dose-length product compared with using organ doses: consequences of adopting International Commission on Radiological Protection publication 103 or dual-energy scanning. *AJR Am J Roentgenol* 2010;194:881-889
23. Boetticher H, Lachmund J, Looe HK, Hoffmann W, Poppe B. 2007 recommendations of the ICRP change basis for estimation of the effective dose: what is the impact on radiation dose assessment of patient and personnel? *Rofo* 2008;180:391-395
24. Prakash P, Kalra MK, Gilman MD, Shepard JA, Digumarthy SR. Is weight-based adjustment of automatic exposure control necessary for the reduction of chest CT radiation dose? *Korean J Radiol* 2010;11:46-53
25. Kalra MK, Dang P, Singh S, Saini S, Shepard JA. In-plane shielding for CT: effect of off-centering, automatic exposure control and shield-to-surface distance. *Korean J Radiol* 2009;10:156-163
26. Kalra MK, Maher MM, Toth TL, Hamberg LM, Blake MA, Shepard JA, et al. Strategies for CT radiation dose optimization. *Radiology* 2004;230:619-628
27. Gallagher MJ, Raff GL. Use of multislice CT for the evaluation of emergency room patients with chest pain: the so-called "triple rule-out". *Catheter Cardiovasc Interv* 2008;71:92-99